ELSEVIER

www.elsevier.nl/locate/ica

Inorganica Chimica Acta 294 (1999) 240–254

Inorganica Chimica Acta

Reactions of H_2, silanes, and olefins with superelectrophilic cationic rhenium complexes: heterolytic cleavage of H_2 and relation to the structure and function of hydrogenases

Jean Huhmann-Vincent, Brian L. Scott, Gregory J. Kubas *

Chemical Science and Technology Division, MS J514, Los Alamos National Laboratory, Los Alamos, NM 87545, USA

Received 14 January 1999; accepted 23 June 1999

Abstract

The reaction of *cis*-$Re(CO)_4(PR_3)Me$ (R = Ph, Cy) with the Lewis acid $B(C_6F_5)_3$ was studied by NMR spectroscopy, and was found to provide an equilibrium mixture of the solvent-coordinated complex [*cis*-$Re(CO)_4(PR_3)(ClCH_2Cl)$][$MeB(C_6F_5)_3$] and the reactants. Reaction of *cis*-$Re(CO)_4(PR_3)Me$ with HX (X = H, $SiEt_3$) in the presence of $B(C_6F_5)_3$ at low temperature yielded the σ-bonded complexes [*cis*-$Re(CO)_4(PR_3)(\eta^2$-HX)][$MeB(C_6F_5)_3$] which decomposed at room temperature via intramolecular heterolytic cleavage of the X–H bond to produce MeX and the hydride-bridged dimer [*cis*-$Re(CO)_4(PR_3)]_2(\mu$-H){$MeB(C_6F_5)_3$}. The unstable H_2 binding and cleavage on this and other highly electrophilic organometallic complexes that contain strong π-acceptor CO ligands can be related to the structure and function of metalloenzymes such as Fe-containing hydrogenases that catalyze $H_2 \leftrightarrow 2H^+ + 2e^-$. The latter contain dinuclear organometallic-like active sites with CO ligands, which would promote binding and heterolytic cleavage of molecular H_2 in biological systems. The Fe–Fe and Ni–Fe bonds in hydrogenases are likely sites for protonation to form a bridging hydride as the initial step in the mechanism of H_2 formation, and electrophilic fragments such as $[Re(CO)_4(L)]^+$ strongly prefer to form bridging rather than terminal hydrides. The reaction of olefins and Et_3SiH with the [*cis*-$Re(CO)_4(PR_3)(ClCH_2Cl)$][BAr_F] ($BAr_F = B[3,5\text{-}(CF_3)_2(C_6H_3)_4^-]$) system was also investigated, and the X-ray crystal structure of the dimer {[*cis*-$Re(CO)_4(PPh_3)]_2(\mu$-H)}{BAr_F} was determined. © 1999 Elsevier Science S.A. All rights reserved.

Keywords: Crystal structures; Rhenium complexes; Silane complexes; Dihydrogen complexes; Olefin complexes

1. Introduction

We are interested in the reactivity of unsaturated transition metal complexes L_nM towards HX σ-bonds, where X = H, Si and C. The interaction between a metal complex and a σ-bond is governed by both the extent of π-backdonation from metal d-orbitals to the σ* antibonding HX orbital ($M_d \rightarrow HX_{\sigma^*}$) and the donation from the HX σ-bonding orbital to an empty metal orbital of appropriate orientation ($HX_\sigma \rightarrow M$) [1]. Both interactions weaken the HX bond. If there is a balance between σ-donation and π-backdonation, a stable σ-complex should form, as in $W(CO)_3(P^iPr_3)_2(\eta^2$-$H_2)$ [2] and $Mo(CO)(diphosphine)_2(\eta^2$-$HSiPhH_2)$ [3]. If the system contains an electron-rich metal in which the predominant interaction is $M_d \rightarrow HX_{\sigma^*}$ backdonation, homolytic cleavage of the H–X bond can occur via oxidative addition, as in $MoH_2(CO)(depe)_2$ versus less electron-rich $Mo(\eta^2$-$H_2)(CO)(dppe)_2$ [1k] and in $[ReH_2(CO)(PMe_3)_4][BF_4]$ [4] (Eq. (1)).

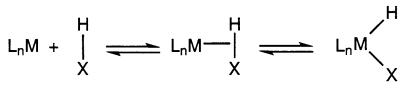

(1)

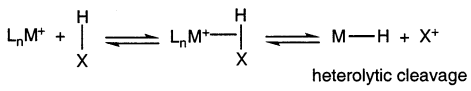

(2)

However, if the system contains an electron-deficient metal which is a poor π-donor (usually cationic) and the predominate interaction is $HX_\sigma \rightarrow > M$ donation,

* Corresponding author. Tel.: +1-505-667 5767; fax: +1-505-667 3314.

PII: S0020-1693(99)00243-1

activation of the H–X bond can occur via heterolytic cleavage (Eq. (2)) because of greatly increased acidity of the HX ligand [1b–d]. For example, [*mer*-$Re(CO)_3(PPh_3)_2(\eta^2\text{-}H_2)]^+$ is deprotonated by strong bases such as 1,8-bis(dimethylamino)naphthalene to form the corresponding neutral [Re]H. As we reported in a preliminary communication, the analogue with CO replacing a phosphine, [*cis*-$Re(CO)_4(PR_3)(\eta^2\text{-}H_2)]$-$[BAr_F]$, contains an even more electrophilic Re^+ center that lowers the pK_a of H_2 in the σ-complex considerably [1k]. The H_2 ligand is deprotonated by weak bases such as $^iPr_2O$, indicating a pK_a of 1 to −2. The Re complex along with Morris and coworkers [5a] very acidic $[Ru(\eta^2\text{-}H_2)(CNH)(dppe)_2]^{2+}$ and Bianchini et al. [5b] unstable $[IrH_2(H_2)(triphos)]^+$ systems are rare examples of organometallic complexes that heterolytically activate H_2 gas [5]. In these systems the pK_a of H_2 is lowered from 37 down to as low as −5, an increase in acidity of 42 orders of magnitude.

An HX bond can be functionalized through either route shown in Eqs. (1) and (2). Although there are many examples of the oxidative addition of H_2 and silanes in electron-rich systems (Eq. (1)) [1,3], well-defined examples of heterolytic σ-bond activation in electron-poor systems (Eq. (2)) seem generally limited to reactions of H_2, and usually require the presence of a relatively good base. In this paper, we describe the reactions of HX (X = H, $SiEt_3$) as well as olefins with the highly electrophilic cationic system [*cis*-$Re(CO)_4(PR_3)]^+$ (R = Ph, Cy). The latter contains mainly π-acceptor CO ligands which enhance the $HX_\sigma \rightarrow M$ σ-donation at the expense of the $M_d \rightarrow HX_{\sigma^*}$ backdonation, and thus heterolytic activation pathways are favored over oxidative addition for both H_2 and silane reactions. The presence of CO ligands also appears to be a critical feature of the active site of hydrogenases [6], particularly in the recently determined structures of Fe-only metalloenzymes, *Clostridium pasteurianum* [6a] and *Desulfovibrio desulfuricans* [6b] which contain dinuclear Fe active sites with CO ligands *cis* and/or *trans* to the putative H_2 binding site. Until the hydrogenases, CO ligands had never been found as intrinsic constituents of a prosthetic group in biology. Apparently their function is to increase the electrophilicity of the Fe site, thereby increasing the lability and acidity of H_2, which promotes heterolytic cleavage and transfer of protons to proximal cysteinyl sulfur ligands. It is also significant that the active site in the crystal structures is occupied by a labile H_2O ligand that has been shown to be competitively displaced by H_2 in organometallic systems [7]. Organometallic chemistry thus perfectly models the enzymatic process that interconverts protons and H_2, as will be discussed in this paper.

2. Results and discussion

2.1. Reaction of *cis*-$Re(CO)_4(PR_3)Me$ (*1*) with $B(C_6F_5)_3$

We have recently demonstrated that the solvento complexes [*cis*-$Re(CO)_4(PR_3)(S)][BAr_F]$ ($BAr_F = [B(3,5\text{-}(CF_3)_2C_6H_3)_4]^-$; R = Ph, ^iPr, Cy; S = OEt_2, $ClCH_2Cl$, and NC_5F_5) are prepared from *cis*-$Re(CO)_4(PR_3)Me$ (**1**) by either methyl abstraction with $[Ph_3C][BAr_F]$ or protonation with $[H(OEt_2)_2][BAr_F]$ in the appropriate solvent [8]. These complexes were characterized structurally, and a brief study of the reaction of [*cis*-$Re(CO)_4(PR_3)(ClCH_2Cl)][BAr_F]$ with H_2 was communicated [1k]. An important feature in this highly electrophilic system is the use of the non-coordinating anion BAr_F^-, which allows for facile substitution of the coordinated solvent molecule with other substrates. The anion-coordinated complexes [*cis*-$Re(CO)_4(PPh_3)(A)]$ have previously been reported by Hope and coworkers ($A = OTeF_5^-$) [9] and Beck and Schweiger ($A = FBF_3^-$) [10].

In the current study, *cis*-$Re(CO)_4(PR_3)Me$ (R = Ph, **1a**; Cy, **1b**) was reacted with the Lewis acid borane $B(C_6F_5)_3$ in CD_2Cl_2 solution and the products were studied by NMR spectroscopy. Here, the generated ionic complex [*cis*-$Re(CO)_4(PR_3)(ClCD_2Cl)][MeB(C_6F_5)_3]$ (R = Ph, **2a**; Cy, **2b**) remained in equilibrium with the starting materials, as shown in Eq. (3).

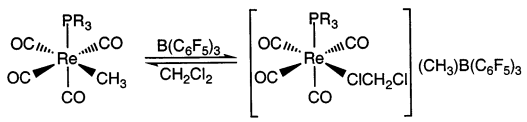

1 2 (3)

For the case where PR_3 is PPh_3, two broad resonances at −0.56 and 0.48 ppm were observed in the room temperature ^1H NMR spectrum and were assigned to the Re*Me* of **1a** and *Me*$B(C_6F_5)_3$ of **2a**, respectively. As the solution was cooled, the intensity of the BMe peak grew and sharpened as the intensity of the ReMe resonance broadened and decreased, as shown in Fig. 1.

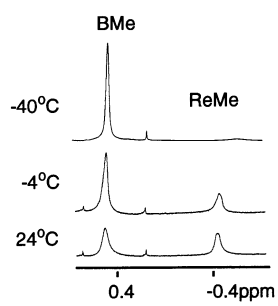

Fig. 1. ^1H NMR (CD_2Cl_2) of *cis*-$Re(CO)_4(PPh_3)$ (**1a**) + $B(C_6F_5)_3$, methyl region.

The thermodynamic parameters for this equilibrium were calculated from the integrated ratio of ReMe and BMe resonances in the ^{1}H NMR spectra as: $\Delta H = -7.1 \pm 0.3$ kcal mol^{-1}, $\Delta S = -24.4 \pm 1.2$ e.u., $\Delta G_{298} = 0.2 \pm 0.3$ kcal mol^{-1}. The fact that **1** remained in equilibrium with **2** at room temperature was unexpected and indicates that the Lewis acidity of the [*cis*-Re(CO)$_4$(PR$_3$)]$^+$ fragment is comparable to that of B(C$_6$F$_5$)$_3$.

For the analogous reaction of B(C$_6$F$_5$)$_3$ with the PCy$_3$ derivative **1b**, one very broad resonance was observed in the ^{1}H NMR spectrum at room temperature at 0.22 ppm, which sharpened and shifted downfield to 0.42 ppm at low temperature. For comparison, the free ReMe complexes **1a** and **1b** exhibit doublets at -0.50 ppm ($J_{HP} = 7.5$ Hz) and -0.49 ppm ($J_{HP} = 6.4$ Hz), respectively in the ^{1}H NMR spectrum in CD$_2$Cl$_2$ at room temperature [8,11]. The room temperature ^{31}P{^{1}H} NMR spectrum of the equimolar mixture of **1a** and B(C$_6$F$_5$)$_3$ in CD$_2$Cl$_2$ solution showed broad, overlapping resonances at 11.1 and 10.4 ppm, and cooling provided one sharp ^{31}P signal at 11.1 ppm. These chemical shifts are similar to the values we reported previously for [*cis*-Re(CO)$_4$(PR$_3$)(ClCD$_2$Cl)][BAr$_F$] (11.1 ppm) and unreacted **1a** (10.1 ppm) [8]. In the corresponding room temperature ^{31}P{^{1}H} spectrum for the PCy$_3$ reaction, one broad resonance was observed at 25.2 ppm, which sharpened and shifted to 25.4 ppm at low temperature. We have observed previously the ^{31}P resonance for [*cis*-Re(CO)$_4$(PCy$_3$)(ClCD$_2$Cl)][BAr$_F$] at 25.5 and 13.1 ppm for **1b** [8]. The [*cis*-Re(CO)$_4$(PR$_3$)(ClCH$_2$Cl)][MeB(C$_6$F$_5$)$_3$] complexes **2a** and **2b** were not isolated due to the formation of oils which could not be purified by crystallization due to the presence of small amounts of impurities ($< 5\%$).

There are reaction pathways other than the equilibrium between **1** and **2** shown in Eq. (3) which could account for these observations in the NMR spectra. A borane Lewis acid can also react with a metal alkyl to form an ion-pair (zwitterionic) complex with M–Me–B interactions. This is the case in the solid state for Marks

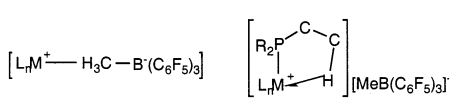

and coworkers' Cp$'_2$ZrMe$^+$MeB(C$_6$F$_5$)$_3^-$ [12] and Schrock and coworkers [NON]ZrMe$^+$MeB(C$_6$F$_5$)$_3^-$ [13]. Furthermore, the formation of an agostic complex is possible in which the vacant site on Re$^+$ center is stabilized by interaction with a C–H bond of a phosphine ligand. This type of interaction is very common and has been observed by X-ray crystallography in the bis-phosphine derivatives [*mer*-M(CO)$_3$(PR$_3$)$_2$][BAr$_F$] (M = Mn [14], Re [1m]). An equilibrium between **1** and either an agostic or zwitterionic complex could lead to broad methyl peaks in the ^{1}H NMR spectra such as those shown in Fig. 1.

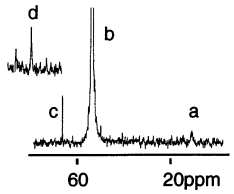

Fig. 2. ^{13}C{^{1}H} NMR (CH$_2$Cl$_2$, -70°C) of *cis*-Re(CO)$_4$(PPh$_3$) (**1a**) + B(C$_6$F$_5$)$_3$, (a) *Me*B(C$_6$F$_5$)$_3$, (b) free *C*H$_2$Cl$_2$, (c) Re–Cl*C*H$_2$Cl. (d) Re–Cl*C*H$_2$Cl, proton coupled, $J_{HC} = 184.3$ Hz.

In order to rule out these possibilities in our Re system and establish that the product **2** is indeed a bound dichloromethane complex, low temperature ^{13}C NMR experiments were conducted. When a CH$_2$Cl$_2$ solution of **1a** and B(C$_6$F$_5$)$_3$ was cooled to -70°C and the ^{13}C{^{1}H} measured, one sharp peak due to bound dichloromethane in Re(Cl*C*H$_2$Cl)$^+$ (**2a**) was observed at 67.0 ppm (Fig. 2). There was also a resonance at 9.4 ppm assigned to Me(B(C$_6$F$_5$)$_3$ which was very broad due to CB coupling. When the proton decoupler was turned off, the peak at 67.0 ppm split into a triplet, with $J_{CH} = 184.6$ Hz, supporting the assignment of this peak as bound CH$_2$Cl$_2$ (free CH$_2$Cl$_2$: δ 54.00 ppm, $J_{CH} = 179.3$ Hz). When the reaction mixture was warmed to room temperature, the peak assigned to bound dichloromethane disappeared due to fast exchange with free CH$_2$Cl$_2$. Similarly, generation of **2b** from **1b** and B(C$_6$F$_5$)$_3$ in CH$_2$Cl$_2$ provided a signal for bound dichloromethane at 67.8 ppm in the ^{13}C{^{1}H} spectrum (-70°C), which split into a triplet ($J_{CH} =$ 186.5 ppm) in the proton-coupled experiment. These results are analogous to those we observed previously for the related BAr$_F^-$ complexes [8]. These observations in the low temperature ^{13}C spectra are also very similar to those observed by Gladysz and coworkers [15] with [Cp$'$Re(NO)(PPh$_3$)(ClCH$_2$Cl)][BF$_4$] in CH$_2$Cl$_2$ at -85°C (78.3 ppm, $J_{CH} = 185.5$ Hz, $J_{CP} =$ 3.8 Hz).

There have recently been a number of examples of isolated complexes with coordinated dichloromethane, most of which are derived from extremely electron-deficient cationic metal centers with low-interacting anions [16]. In the complexes characterized by X-ray crystallography, dichloromethane has been found to coordinate bidentate through the chloride atoms in Ag$_2$(CH$_2$Cl$_2$)$_4$Pd(OTeF$_5$) [17] and [RuH(CO)(CH$_2$Cl$_2$)(P^{t}Bu$_2$Me)$_2$][BAr$_F$] [18] and monodentate through one of the chloride atoms in [*cis*-Re(CO)$_4$(PR$_3$)][BAr$_F$] (R = Ph, ^{i}Pr) [8], [PtAg(CH$_2$Cl$_2$)(C$_6$F$_5$)$_2$(acac)]$_2$ [19], [Cp*Ir(Me)(PMe$_3$)(ClCH$_2$Cl)][BAr$_F$] [20] and [*trans*-

$PtH(P^iPr_3)_2(ClCH_2Cl)][BAr_F]$ [21]. The coordinated dichloromethane in $[CpMo(CO)_3(ClCH_2Cl)][PF_6]$ [22] and $[Cp'Re(NO)(PPh_3)(ClCH_2Cl)][BF_4]$ [15] has been assigned on the basis of IR spectral data and low temperature ^{13}C NMR spectral data, respectively.

2.2. Reaction of $[cis\text{-}Re(CO)_4(PR_3)(ClCH_2Cl)][MeB(C_6F_F)_3]$ (2) with H_2, HD and D_2

Despite the lability of the dichloromethane ligand of **2** in CD_2Cl_2 solution, only weak binding to H_2 was observed due to fast exchange with free CD_2Cl_2. A CD_2Cl_2 solution of **1** and $B(C_6F_5)_3$ was frozen in a J-Young NMR tube at liq. N_2 temperature, placed under approximately 3 atm of H_2, and inserted into a pre-cooled NMR spectrometer probe (-70°C). At low temperatures (-70 to -40°C), the σ-complex [*cis*-$Re(CO)_4(PR_3)(\eta^2\text{-}H_2)][MeB(C_6F_5)_3]$ (R = Ph, **3a**; Cy, **3b**) was observed in low concentrations (< 5%), identified by the broad resonance in the ^1H NMR spectra at -4.2 and -4.6 ppm for **3a** and **3b**, respectively. The ^1H and $^{31}P\{^1H\}$ NMR spectra were comparable to those we could observe at room temperature for the more stable analogue with the BAr_F^- anion in the less coordinating solvent C_6D_5F [1k].

When the analogous reactions are performed with HD, the upfield resonances at -4.2 and -4.6 ppm in the ^1H NMR spectra split into triplets with $J_{HD} = 33.9$ and 33.6 Hz, respectively, confirming the presence of a σ-complex. The high J_{HD} observed for these complexes is consistent with a highly electrophilic cationic $M(\eta^2\text{-}H_2)$ system [23] and suggests a short H–H bonding distance (0.85–0.87 Å) based on Morris and coworkers and Luther and Heinekey's correlations [24]. This is consistent with a bonding picture in which the $H_2 \rightarrow M$ σ-bonding interaction is enhanced at the expense of $M \rightarrow H_2$ backbonding [23a,b,e]. It is also instructive to note that the electronic nature of the ligand(s) *cis* to H_2 (PCy_3 versus PPh_3 in **3**) usually has very little effect on J_{HD} and the H–H distance, especially when H_2 is *trans* to CO, as chronicled previously [23e]. Fig. 3 shows the $Re(\eta^2\text{-}HD)$ region of the ^1H NMR spectrum for the BAr_F^- analogue of **3a**. No HP coupling is observed and the broad hump under the triplet is due to the presence of a small amount of $Re(\eta^2\text{-}H_2)$.

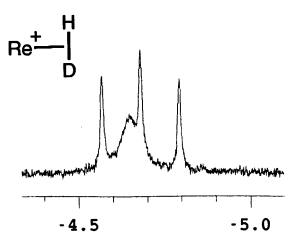

Fig. 3. ^1H NMR (C_6D_5F, -40°C) [*cis*-$Re(CO)_4(PPh_3)(\eta^2\text{-}HD)][BAr_F]$, hydride region, $J_{HD} = 33.9$ Hz.

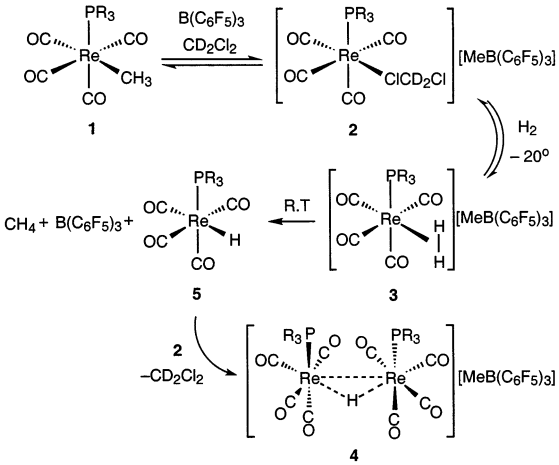

Scheme 1. Heterolytic cleavage of H_2.

Interestingly, when CD_2Cl_2 solutions of [*cis*-$Re(CO)_4(PR_3)(\eta^2\text{-}H_2)][MeB(C_6F_5)_3]$ were warmed above -40°C, the formation of CH_4 was observed in the ^1H NMR spectra along with an upfield triplet at -15.6 ppm (R = Ph, $J_{HP} = 10.0$ Hz) or -17.6 ppm (R = Cy, $J_{HP} = 7.8$ Hz) that was assigned to the hydride-bridged dimer $\{[cis\text{-}Re(CO)_4(PR_3)]_2(\mu\text{-}H)\}\{MeB(C_6F_5)_3\}$ (R = Ph, **4a**; Cy, **4b**). At room temperature the only products observed in the ^1H NMR spectra were the hydride-bridged dimer and methane. There was only one resonance in the ^{31}P NMR spectra (1.9 ppm, **4a**; 13.7 ppm, **4b**), indicating complete conversion to the dimer at room temperature. The reaction of **1** with $B(C_6F_5)_3$ and H_2 was also carried out in C_6D_5F, and warming above -20°C also proceeded with the generation of CH_4 and the hydride-bridged dimer **4**. One proposed reaction pathway for an intramolecular heterolytic cleavage of H_2 which involves the borane anion is shown in Scheme 1 for the CD_2Cl_2 solution case.

Direct protonation of the anion $MeB(C_6F_5)_3$ by the acidic H_2 in **3** would form methane, $B(C_6F_5)_3$, and the rhenium hydride *cis*-$Re(CO)_4(PR_3)H$ (R = Ph, **5a**; Cy, **5b**). Compound **5** is not observed in the ^1H NMR spectra, but presumably quickly reacts with unreacted **2** (or **3**) to form the hydride-bridged dimer **4**, which appears to be a 'thermodynamic sink' in these systems. Such protonation of a borane anion has precedence as shown in Eq. (4) where the H_2 complex is also unstable and is generated from H_2 gas [5b].

$$[IrH_2(H_2)(triphos)]^+[BPh_4]^- \rightarrow IrH_3(triphos) + BPh_3 + benzene \quad (4)$$

Another example of anion protonation by an H_2 ligand occurs in $[Ru(H_2)(CNH)(dppe)_2][OTf]_2$ which eliminates triflic acid, a remarkable example of heterolytic activation of H_2 gas to form a strong acid [5a]. In this case the acidity of H_2 is increased approximately 42

orders of magnitude on binding to Ru (pK_a of free H_2 is 37 and -5 when bound). Another scenario in Scheme 1 is intermolecular heterolytic cleavage of H_2, e.g. protonation of the Me group in equilibrium quantities of **1** by the acidic H_2 in **3** to give CH_4, **2**, and **5**. Although not able to distinguish between the two mechanisms, a reaction sequence carried out using D_2 instead of H_2 generates CH_3D as observed in the ^1H NMR spectrum. The room temperature ^{31}P spectra for the H_2 and D_2 reactions are virtually identical, indicating the formation of the deuteride-bridged dimer. Finally, no scrambling of protons into the Re–D–Re dimer was observed.

This facile heterolytic activation of H_2 is indicative of a very electrophilic Re^+ center which lowers the pK_a of H_2 in the σ-complex considerably. In the analogous BAr_F^- system, the σ-complex [*cis*-$Re(CO)_4(PR_3)(\eta^2\text{-}H_2)$][$BAr_F$] was stable at room temperature, but addition of the weak base $^iPr_2O$ resulted in the formation of [$H(O^iPr_2)_2$][BAr_F] and **4**. The pK_a of $^iPr_2O$ has not been reported, but the pK_a values of Et_2OH^+ and Me_2OH^+ in aqueous sulfuric acid are -2.4 and -2.5, respectively [25], therefore the pK_a of [*cis*-$Re(CO)_4(PR_3)(\eta^2\text{-}H_2)$][A] can be estimated as approximately 1 to -2 [1k].

This type of activation of H_2 by an electrophilic transition metal complex has been observed in the case of [$Cp^*Ru(CO)_2(\eta^2\text{-}H_2)$][$BF_4$], which protonates Et_2O to form [$H(OEt_2)$][BF_4] and the hydride-bridged dimer {[$Cp^*Ru(CO)_2$]$_2$(μ-H)}{BF_4} [26]. The pK_a values of $M(\eta^2\text{-}H_2)$ σ-complexes have been measured over a range of approximately -3 to $+17$ for monocationic complexes, and as low as -6 for dicationic Ru, Os, and Fe complexes [1c,j,23b,d,24].

2.3. Comparison of heterolytic splitting of H_2 on electrophilic organometallic and hydrogenase sites

As mentioned in Section 1, there is a close relationship between the heterolytic activation of H_2 [27] in CO-containing organometallic complexes such as $[Re(CO)_4(PR_3)(\eta^2\text{-}H_2)]^+$ and biological enzymes such as hydrogenases and possibly nitrogenases as well. As originally noted by Crabtree [28], several properties of H_2 ligands such as their acidity and ability to compete with N_2 ligands clearly is relevant to the structure and function of these enzymes. Hydrogenases are redox enzymes where the H_2 molecule is split heterolytically, thus catalyzing the interconversion of H_2 and protons to either utilize H_2 as an energy source or dispose excess electrons as H_2 [29].

$$H_2 \leftrightarrow 2H^+ + 2e^- \quad (5)$$

These enzymes are incredibly efficient (10^9 turnovers/h) and crucial to hydrogen metabolism essential to many microorganisms of immense biotechnological interest such as methanogenic, acetogenic, nitrogen-fixing, photosynthetic, and sulfate-reducing bacteria. Several types of hydrogenases have been identified, where the apparent active site contains either nickel in combination with iron [Ni–Fe], iron-only (e.g. *Clostridium pasteurianum*), or remarkably, no transition metals at all. The latter, found in methanogenic archaea, *Methanobacterium Thermoautotrophicum*, appears to be a purely organic hydrogenation catalyst, promoting the reduction of a pterin compound by H_2 and also producing a proton, as a step in methane formation from CO_2 and H_2 [30]. One proposed mechanism is analogous to that of Olah et al. [31] for the reversible formation of carbocations and H_2 from alkanes in superacid media, e.g. Eq. (6):

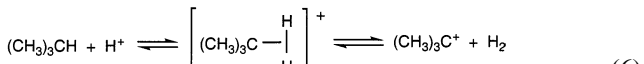

(6)

This would indicate that a highly electrophilic site is critical to H_2 activation, which is supported by ab initio studies [32]. In this context, R_3C^+ and 16e metal centers such as $[Re(CO)_4(PR_3)]^+$ are strongly electrophilic isolobal fragments. The recent exciting discovery of the unprecedented biological presence of CO ligands in metal-containing hydrogenases [6,33] would appear to relate to the function of π-acceptors in increasing the electrophilicity of the active site, thereby enhancing intramolecular heterolysis of H_2 as in carbonyl-rich $[Re(CO)_4(PR_3)(\eta^2\text{-}H_2)][MeB(C_6F_5)_3]$ in Scheme 1. Both experimental [34] and theoretical [35,36] models have been proposed for the active sites of [NiFe] hydrogenases based on $[Fe(CO)(CN)_2]$ cores since Fe-bound cyanide is also found in hydrogenases and is difficult to distinguish from CO crystallographically. It should be emphasized however that the negatively-charged cyanide ligand is not a very good π-acceptor but a strong σ-donor more like chloride or thiolate [1n]. Thus, it is undoubtedly the CO ligand(s) that is crucial in controlling H_2 binding and activation in hydrogenases. Importantly, electrophilic metal sites with such electron-withdrawing ligands also can greatly favor H_2 binding over N_2 binding, particularly when coordinated *trans* to CO [14].

The recent crystal structures of *C. pasteurianum* (1.8 Å resolution) and *Desulfovibrio desulfuricans* (1.6 Å) are quite revealing as to the remarkable similarity between dihydrogen activation on organometallic centers and biological systems such as hydrogenases. In the former enzyme, five CO and/or CN ligands were identified to be bound to a dinuclear iron center, including one in a bridging position along with two bridging SR ligands [6a]. An electron-transfer Fe_4S_4 'cubane' cluster was attached to Fe(1) via a cysteine thiol bridge as shown below in **6**, which represents one possible structure of the active site with one CN and 4CO (alternatively replacement of a CO on Fe(2) with CN would give a neutral Fe center).

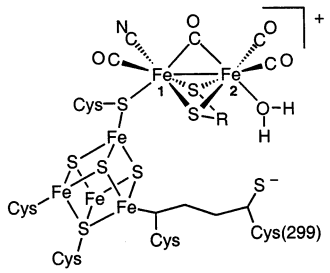

6

Cationic and dicationic Fe–H_2 complexes with CN and CO ligands are known, e.g. $[Fe(H_2)(CN)(depe)_2]^+$ and $[Fe(H_2)(CO)(depe)_2]^{2+}$, and the CN ligand can be protonated to CNH [23b,f]. It is reasonably clear that the bridging diatomic carbon ligand is CO and not CN, which does not bridge through carbon only (μ-CNH may be possible). This is crucial because it places CO *trans* to the aquo ligand located crystallographically on Fe(2), a rare configuration even in organometallic chemistry but well exemplified by $W(CO)_3(PR_3)_2(H_2O)$ [7a]. As we have shown, H_2 can displace H_2O on this tungsten center, and H_2 binding is actually favored at ambient temperature by 1–2 kcal mol^{-1} in terms of ΔG, indicating that in *C. pasteurianum* the probable site for H_2 binding/elimination is *trans* to the μ-CO, as also proposed by Peters et al. [6a]. Importantly, CO labilizes the ligand *trans* to it, especially H_2 [23e], which is critical for reversible binding and elimination of H_2 from the active site. The more electrophilic cationic Re fragment $[Re(CO)_4(PR_3)]^+$ also coordinates H_2O *trans* to CO, although the aquo ligand is less labile than in the neutral W complex and is more strongly bound than ethers or CH_2Cl_2 [8]. Strong π-acceptors also greatly increase the acidity of metal-bound H_2, particularly when *trans* but also when *cis* to H_2. Thus, the $[Re–H_2]^+$ complex **3** is much more easily deprotonated than the W–H_2 species, which requires a strong base [37]. In the hydrogenases, it is likely that the Fe active site is intermediate in electrophilicity but closer to that of **3**. The active site of *D. desulfuricans* is similar to that of *C. pasteurianum*, but a bridging CO ligand was not located in the crystal structure. An aquo ligand (or other monatomic oxygen species such as OH) on Fe(2) was present, although it is not clear if it is bridging or terminal, and Fe(2) was proposed to be coordinatively unsaturated [6b]. A 1,3-propanedithiol ligand was identified to bridge the irons, similar to the bridging thiols in **6** (where R could be $–CH_2CH_2CH_2–$). Assuming the crystallography is accurate, it is possible that different enzymes have evolved with stereochemically distinct active sites. Also, reorientation of a terminal CO to a bridging position and other ligand rearrangements are very facile in organometallic systems (equilibrium process in many cases), so in the actual mechanistic steps H_2 ligand(s) could be positioned *trans* to a variety of

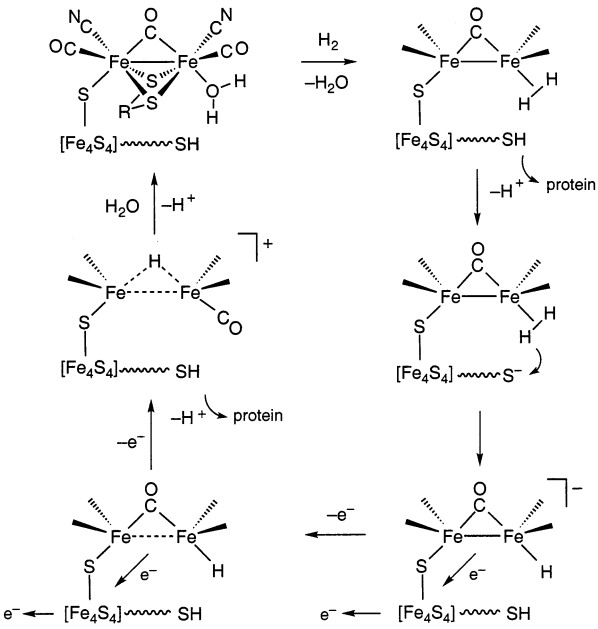

Scheme 2.

ligands. The number of structural and mechanistic possibilities on this remarkably versatile dinuclear site is immense, especially when other variables such as Fe–Fe bonding are taken into account. Because the *trans* effect is so important in H_2 activation, the active site has a tremendous range of flexibility for either consuming or releasing H_2 (Eq. (5) is reversible in most hydrogenases). The acidity of H_2 can be adjusted easily to suit physiological conditions and the relatively low redox potentials typical of these active sites.

Scheme 2 presents one (of many) reasonable mechanism for reversible H_2 consumption/production on *C. pasteurianum*, the basic principles of which could be applied to other enzymes.

The bridging dithiolate is not shown throughout for clarity. Although the dinuclear center could be cationic as shown in **6** for ease of heterolysis of H_2 in direct comparison with organometallic systems such as **3** (Scheme 1), Scheme 2 assumes perhaps more reasonably that one CN is present on each Fe, i.e. a neutral Fe(II) center. It is important to note that such a variation does not change the oxidation state of the irons, which is generally believed to be Fe(II) in all states of the hydrogenases, and a low spin d^6 Fe(II) octahedral configuration is well-known to favor H_2 binding [1]. Thus, the function of the unusual CO and CN ligands must be to maintain this spin state and an electron-poor metal center.

An Fe–Fe bond is present in both enzymes based on crystallographic Fe–Fe distances of approximately 2.6 Å that are typical for a dithio-bridged Fe–Fe system [38], as exemplified by the CpFe–CN complex we reported many years ago [38a].

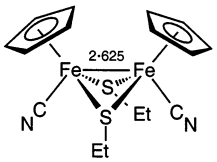

The structures in Scheme 2 would give the proper 34e count for an octahedral Fe–Fe bonded system (assuming a dative 2e interaction between S_{cubane} and Fe(1)). Transfer of a proton from the cationic Fe–H_2 species could readily occur as in Scheme 1, except here the proton jumps to a deprotonated cysteine(299) sulfur site located conveniently in close proximity (3 Å) to the H_2 binding site (structure **6**). Both Crabtree and Morris and coworkers [39] have demonstrated that such intramolecular heterolytic cleavage occurs readily, as exemplified by Eq. (7).

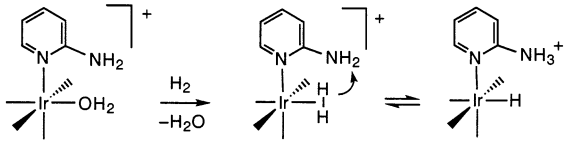

(7)

Although the crystal structure of *D. desulfuricans* did not show an adjacent cysteine, a lysine residue is near to Fe(2). The next steps involve movement of protons away from the active site to the protein and synchronous or asynchronous electron transfer to the cubane cluster and then away from the site via other Fe–S clusters. Thus, the electrons originally present on H_2 could flow through the Fe–Fe bond and, depending on whether a one- or two-electron transfer process takes place, one-electron Fe···Fe bonds [38b] may be present in the intermediates (shown in Scheme 2 for one-electron transfer steps). These bonds are characterized by Fe–Fe distances of 2.9–3.1 Å, as exemplified by $[Cp_2Fe_2(\mu\text{-}S_2)(\mu\text{-}SEt)_2]^+$ [38,40]. The high flexibility of the Fe–Fe separation (2.6–3.2 Å) and the directly-related degree of Fe–Fe interaction (zero-, one-, or two-electron bonds) would be expected to facilitate the electron/proton transfer processes. This may apply to the [NiFe] hydrogenases as well, which also have bridging SR groups and Ni–Fe separations of 2.55 Å in the active site of *Desulfovibrio vulgaris* and 2.9 Å in the inactive, oxidized form of *Desulfovibrio gigas* [41].

The reverse reaction, formation of hydrogen gas from H^+ and electrons, is interesting from the standpoint of the mechanism of initial protonation of the Fe center to form a metal hydride. Protonation of a 16e metal center is extremely rare and paradoxical because it represents reaction of two Lewis acids, the metallo-Lewis acid and H^+. However 16e $W(CO)_3(PR_3)_2$ (which contains an agostic C–H interaction but effectively has a vacant d-orbital) was found to be protonated by strong acids such as $HBF_4{\cdot}Et_2O$ to give $WH(BF_4)(CO)_3(PR_3)_2$ [42]. Another more basic and presumably more likely site for protonation in the enzyme active sites would be the electrons in the Fe–Fe and Ni–Fe bonds. The proximal cysteine(299) could transfer its proton to the M–M bond for example. Metal–metal bonds can readily be reversibly protonated to form hydride-bridged species [43], and electrophilic systems show a tendency to form μ-H structures as exemplified above by $\{[Re(CO)_4(PR_3)]_2(\mu\text{-}H)\}^+$ (**4**). The Fe–Fe bond in $[CpFe(CO)(PR_3)(\mu\text{-}CO)]_2$ is as basic as weak amines (pK_b around 6) and concomitant shift of bridging CO to terminal positions occurs (Eq. (8)) [44]. Protonation of the Fe–Fe bond in $[Fe(CO)_2(PR_3)(\mu\text{-}SR')]_2$ takes place in preference to protonation of the sulfur ligands (Eq. (9)) [45].

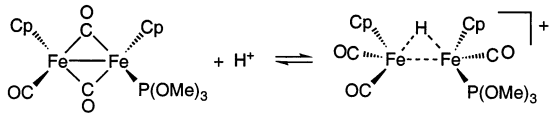

(8)

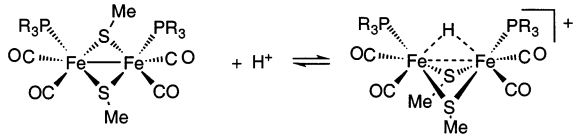

(9)

The basicities of M–M bonds such as in $[CpRu(CO)_2]_2$ were shown to be substantially higher than that of the metal sites in related 18e mononuclear complexes and are highly sensitive to the nature of the ancillary ligands [43]. Theoretical studies of [NiFe] hydrogenase mechanisms indicate that hydride-bridged intermediates are energetically favorable [35,36]. ENDOR studies indicate that two types of exchangeable hydrogen nuclei are present in the vicinity of the Ni ligands in the Ni–C active form of the [NiFe] enzyme [46], consistent with the proposal of a μ-H ligand [41c]. The bridging hydride could easily revert to a terminal hydride on electron transfer, displacing the aquo ligand, as shown in the reverse sequence of Scheme 2. The terminal hydride could then be protonated to a labile H_2 ligand that is readily displaceable by water, and the cycle would continue. Formation of a bridging H_2 ligand is conceivable although a μ-H_2 ligand has not been confirmed structurally.

*2.4. Preparation and X-ray structure of {[cis-Re(CO)$_4$(PR$_3$)]$_2$(μ-H)}{BAr$_F$} (**4**)*

In order to verify the identity of the thermodynamically favored hydride-bridged dimer **4** as the product from the heterolytic activation of H_2 as shown in Scheme 1, authentic samples of $\{[cis\text{-}Re(CO)_4(PR_3)]_2(\mu\text{-}H)\}\{BAr_F\}$ (R = Ph, **4a′**; Cy, **4b′**) were prepared. One equiv. of $[H(OEt_2)_2][BAr_F]$ was added to an Et_2O solution of **1a**, resulting in the evolution of CH_4 and the formation of the ether complex $[cis\text{-}Re(CO)_4(PPh_3)(OEt_2)][BAr_F]$. Subsequent addition of one equiv. of **5a**

Table 1
Crystal data and structure refinement for **4a′** [a]

Chemical formula	$C_{76}H_{43}BF_{24}O_8P_2$
Formula weight	1985.25
Temperature (°C)	−75
Wavelength (Å)	0.71073
Space group	$P2_1/c$
a (Å)	17.752(3)
b (Å)	22.295(2)
c (Å)	19.268(4)
β (°)	103.05(2)
V (Å^3)	7429(2)
Z	4
D_{calc} (g cm^{-1})	1.775
μ (cm^{-1})	0.3415
Final R indices	$R_1 = 0.0539$, $wR_2 = 0.0986$

[a] $R_1 = \sigma \||F_o|-|F_c|\|/\sigma |F_o|$ and $wR_2 = [\Sigma[w(F_o^2-F_c^2)^2]/\Sigma[w(F_o^2)^2]]^{1/2}$. The parameter $w = 1/[\sigma^2(F_o^2)+(0.0348P)^2+19.4218P]$.

provided the hydride-bridged dimer **4a′**, which was isolated in high yield (92%) as large colorless crystals by addition of hexanes. The PCy_3 analogue **4b′** was prepared in a similar fashion from **1b**, **5b**, and $[H(OEt_2)_2][BAr_F]$, and isolated in an 82% overall yield (Eq. (10)).

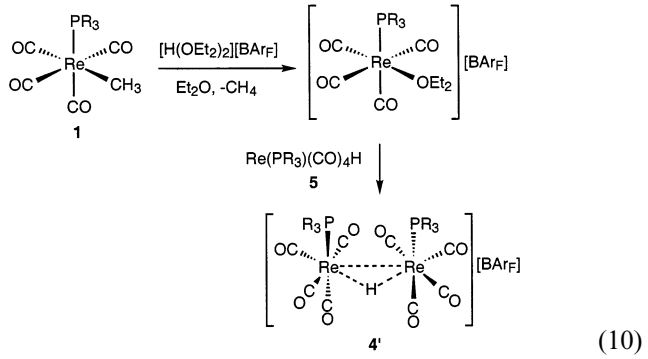

(10)

The ^{1}H NMR spectra of **4a′** and **4b′** in CD_2Cl_2 solution showed upfield triplets at exactly the same chemical shift as those observed in the H_2 heterolytic activation experiments described above with either the BAr_F^- or the $MeB(C_6F_5)_3^-$ anion. The ^{31}P NMR spectra showed one resonance at 1.9 ppm for **4a′** and 13.7 ppm for **4b′**, which are at identical chemical shifts to those observed for the $MeB(C_6F_5)_3^-$ derivatives. These hydride-bridged dimers were stable indefinitely in Et_2O solution, but decomposed slowly in CD_2Cl_2 solution (approximately 40% in 5 days) to the chloride-bridged dimers $\{[cis\text{-}Re(CO)_4(PR_3)]_2(\mu\text{-}Cl)\}\{BAr_F\}$. Addition of a five-fold excess of $[H(OEt_2)_2][BAr_F]$ to a CD_2Cl_2 solution of **4a′** did not lead to protonation of the bridged hydride, although addition of 5 equiv. of $[Ph_3C][BAr_F]$ did provide approximately 30% conversion in 15 min to the dichloromethane complex and Ph_3CH.

Crystals of **4a′** suitable for X-ray diffraction studies were obtained by slow diffusion of hexanes into a Et_2O solution. Table 1 lists a summary of crystallographic data, selected bond lengths and angles can be found in Table 2, the atomic coordinates are in Table 3, and an ORTEP diagram is shown in Fig. 4. The ORTEP shows that the *cis* configuration of phosphine and hydride is retained, and the environment about each Re center is octahedral. The position of the bridged hydride was refined and the average Re–H distance is 1.91 Å. The Re–H–Re angle is 124(2)°, which is similar to the angle we previously observed for the chloride-bridged dimers $\{[cis\text{-}Re(CO)_4(PR_3)]_2(\mu\text{-}Cl)\}\{BAr_F\}$ (R = Ph, 128.2(2)°; Cy, 123.85(2)°) [8]. The Re–Re separation in **4a′** is 3.380 Å, which is considerably shorter than those observed for the chloride-bridged dimers, 4.333 and 4.460 Å, respectively for R = Ph and Cy. This reflects the two-electron, three-center nature of the bonding in M–μ-H–M complexes (denoted by dashed lines). There are no short interactions observed between the cation dimer and the BAr_F^- anion.

Table 2
Selected bond lengths (Å) and angles (°) for **4a′**

Bond lengths			
Re(1)–Re(2)	3.330	Re(2)–H	1.90(10)
Re(1)–H	1.92(10)	Re(2)–P(2)	2.500(2)
Re(1)–P(1)	2.504(2)	Re(2)–C(5)	2.009(11)
Re(1)–C(1)	1.994(10)	Re(2)–C(6)	1.949(11)
Re(1)–C(2)	1.941(10)	Re(2)–C(7)	2.010(12)
Re(1)–C(3)	1.994(11)	Re(2)–C(8)	1.936(10)
Re(1)–C(4)	1.947(11)		
Bond angles			
Re(1)–H–Re(2)	124(2)	P(2)–Re(2)–H	89(3)
P(1)–Re(1)–H	84(3)	P(2)–Re(2)–C(6)	169.0(3)
P(1)–Re(1)–C(4)	172.3(3)	C(8)–Re(2)–H	167(3)
C(2)–Re(1)–H	169(3)	C(5)–Re(2)–C(7)	174.7(4)
C(1)–Re(1)–C(3)	174.0(4)		

2.5. Reaction of [cis-Re(CO)$_4$(PR$_3$)(ClCH$_2$Cl)][A] with Et$_3$SiH

Approximately 1 equiv. of Et_3SiH was added to a cooled (−40°C) CD_2Cl_2 solution of **4** and the reaction was monitored by NMR spectroscopy. Between −40 and −20°C the only product observed was the σ-bound silane complex $[cis\text{-}Re(CO)_4(PR_3)(\eta^2\text{-}HSiEt_3)][MeB(C_6F_5)_3]$ (R = Ph, **6a**; Cy, **6b**). The assignment of this product as $Re(\eta^2\text{-}HSiEt_3)$ was made on the basis of an upfield doublet at −8.89 ppm (J_{HP} = 10.5 Hz, **6a**) and −9.41 ppm (J_{HP} = 9.3 Hz, **6b**) which had ^{29}Si satellites (J_{HSi} = 60.9 Hz, **6a**; 61.6 Hz, **6b**). These J_{HSi} fall in the range of values (20–70 Hz) typically found for known σ-bound SiH complexes [3]. Furthermore, the values of the J_{HP} coupling constants for these doublets are too small to be due to a Re–H complex (J_{HP} = 21.9 Hz for **5b**).

As the NMR sample was warmed to 0°C, the intensity of the σ-complex decreased and new resonances

Table 3
Atomic coordinates ($\times 10^4$) and equivalent isotropic displacement parameters ($Å^2 \times 10^3$) for **4a**′

	x	y	z	U_{eq} [a]
Re(1)	1410(1)	1421(1)	4292(1)	30(1)
Re(2)	1284(1)	2903(1)	3917(1)	30(1)
P(1)	2633(1)	1015(1)	4035(1)	30(1)
P(2)	2447(1)	3493(1)	4517(1)	31(1)
B(1)	2529(5)	7037(4)	3046(5)	23(2)
C(1)	1023(5)	1419(4)	3237(5)	37(2)
C(2)	1154(5)	593(4)	4449(5)	38(2)
C(3)	1837(6)	1509(4)	5337(6)	43(3)
C(4)	394(6)	1634(4)	4442(5)	41(2)
C(5)	1696(6)	2794(4)	3036(6)	39(2)
C(6)	292(6)	2593(5)	3391(5)	42(3)
C(7)	904(6)	2935(4)	4823(6)	45(3)
C(8)	872(6)	3675(5)	3558(5)	47(3)
C(9)	3048(3)	1487(2)	3446(3)	31(2)
C(10)	3557(3)	1945(3)	3727(2)	37(2)
C(11)	3878(3)	2302(2)	3278(4)	44(3)
C(12)	3690(4)	2202(3)	2547(3)	61(3)
C(13)	3181(4)	1744(3)	2266(2)	57(3)
C(14)	2860(3)	1386(3)	2715(3)	45(2)
C(15)	2503(4)	275(2)	3579(3)	37(2)
C(16)	1790(3)	91(2)	3177(3)	42(2)
C(17)	1716(3)	−468(3)	2848(3)	45(3)
C(18)	2355(4)	−842(2)	2922(3)	48(3)
C(19)	3069(3)	−658(3)	3325(4)	65(3)
C(20)	3143(3)	−99(3)	3654(3)	56(3)
C(21)	3419(3)	840(3)	4801(3)	34(2)
C(22)	3213(3)	569(3)	5382(3)	41(2)
C(23)	3783(4)	383(3)	5962(3)	54(3)
C(24)	4558(3)	468(3)	5961(3)	59(3)
C(25)	4764(3)	738(3)	5381(3)	51(3)
C(26)	4194(3)	924(3)	4801(3)	38(2)
C(27)	2720(3)	3988(2)	3856(3)	29(2)
C(28)	2505(3)	4589(2)	3814(3)	33(2)
C(29)	2647(3)	4945(2)	3266(3)	41(2)
C(30)	3004(4)	4700(2)	2759(3)	42(2)
C(31)	3219(4)	4099(3)	2801(3)	52(3)
C(32)	3077(3)	3743(2)	3350(3)	38(2)
C(33)	3321(3)	3090(2)	4961(3)	35(2)
C(34)	4054(3)	3236(2)	4870(3)	45(3)
C(35)	4692(3)	2906(3)	5219(4)	57(3)
C(36)	4597(3)	2430(3)	5658(3)	56(3)
C(37)	3864(4)	2285(2)	5748(3)	47(3)
C(38)	3226(3)	2615(3)	5399(3)	36(2)
C(39)	2295(4)	4016(2)	5209(3)	34(2)
C(40)	1567(3)	4261(3)	5175(3)	46(3)
C(41)	1470(4)	4702(3)	5657(4)	58(3)
C(42)	2101(5)	4899(3)	6173(3)	61(3)
C(43)	2828(4)	4654(3)	6207(3)	56(3)
C(44)	2925(3)	4213(3)	5725(3)	44(3)
C(46)	3387(5)	6332(4)	4039(4)	32(2)
C(47)	3933(5)	5895(4)	4261(5)	33(2)
C(48)	4414(5)	5710(4)	3830(5)	33(2)
C(49)	4321(5)	5972(4)	3171(5)	31(2)
C(50)	3777(5)	6408(4)	2951(4)	28(2)
C(51)	1855(5)	6528(4)	2780(4)	25(2)
C(52)	1362(5)	6346(4)	3208(4)	28(2)
C(53)	862(5)	5862(4)	3042(4)	28(2)
C(54)	826(5)	5548(4)	2415(5)	32(2)
C(55)	1297(5)	5730(4)	1977(4)	24(2)
C(56)	1788(5)	6214(4)	2149(4)	28(2)
C(57)	2686(5)	7476(3)	2412(4)	24(2)
C(58)	3391(5)	7771(4)	2493(5)	33(2)
C(59)	3535(5)	8204(4)	2026(5)	35(2)
C(60)	2954(6)	8356(4)	1431(5)	38(2)
C(61)	2246(5)	8074(4)	1335(5)	35(2)
C(62)	2124(5)	7639(4)	1819(4)	30(2)
C(63)	2302(5)	7504(4)	3631(4)	28(2)
C(64)	1559(5)	7746(4)	3505(5)	30(2)
C(65)	1356(5)	8181(4)	3945(5)	33(2)
C(66)	1887(6)	8401(4)	4525(5)	41(2)
C(67)	2631(6)	8161(4)	4662(5)	39(2)
C(68)	2829(6)	7733(4)	4219(5)	37(2)
C(47A)	3996(6)	5597(5)	4967(5)	45(3)
C(49A)	4830(6)	5772(5)	2699(6)	45(3)
C(53A)	383(5)	5666(4)	3547(5)	36(2)
C(55A)	1271(6)	5385(4)	1307(5)	39(2)
C(59A)	4300(6)	8507(5)	2114(6)	53(3)
C(61A)	1606(6)	8246(5)	727(5)	47(3)
C(65A)	539(6)	8399(5)	3760(6)	52(3)
C(67A)	3197(7)	8386(6)	5276(6)	53(3)
F(1)	3363(4)	5654(3)	5224(3)	67(2)
F(2)	4130(3)	5002(3)	4949(3)	57(2)
F(3)	4588(5)	5804(3)	5458(3)	91(3)
F(4)	4837(6)	5196(3)	2604(5)	129(4)
F(5)	4644(6)	5959(5)	2061(4)	150(5)
F(6)	5539(5)	5888(6)	2927(5)	161(5)
F(7)	104(3)	6135(2)	3856(3)	50(2)
F(8)	795(3)	5340(3)	4087(3)	57(2)
F(9)	−231(3)	5337(3)	3246(3)	51(2)
F(10)	1258(8)	4817(3)	1369(4)	154(5)
F(11)	1837(6)	5455(5)	1031(5)	172(6)
F(12)	169(6)	809(4)	5484(5)	695(6)
F(13)	4248(4)	9093(3)	2027(4)	75(2)
F(14)	4747(4)	8408(4)	2758(4)	121(4)
F(15)	4696(4)	8320(3)	1654(5)	95(3)
F(16)	1225(5)	7792(3)	408(4)	110(3)
F(17)	1807(4)	8563(4)	239(4)	122(4)
F(18)	1074(5)	8562(5)	925(4)	136(4)
F(19)	34(4)	7997(3)	3879(4)	80(2)
F(20)	303(4)	8546(3)	3081(3)	74(2)
F(21)	429(4)	8879(3)	4138(4)	81(2)
F(22)	3059(6)	8343(7)	5857(4)	192(7)
F(23)	3865(6)	8214(8)	5339(7)	247(10)
F(24)	3325(9)	8947(5)	5272(6)	211(7)
O(1)	822(4)	1441(3)	2635(4)	52(2)
O(2)	1008(4)	107(3)	4538(4)	60(2)
O(3)	2048 (5)	1579 (3)	5929(4)	62(2)
O(4)	−223(4)	1739(3)	4499(4)	62(2)
O(5)	1860(5)	2735(3)	2511(4)	59(2)
O(6)	−288(4)	2427(3)	3061(4)	51(2)
O(7)	686(5)	2950(3)	5329(4)	65(2)
O(8)	599(5)	4111(3)	3328(4)	67(2)

[a] U_{eq} is defined as one third of the trace of the orthogonalized U_{ij} tensor.

corresponding to the hydride complex **5** and the hydride-bridged dimer **4** began to grow in. At room temperature the ^{31}P and ^{1}H NMR spectra corresponded to complete conversion to dimer **4**, and resonances in the ^{1}H NMR spectrum corresponded to the formation of the silane Et_3SiMe. GC/MS analysis confirmed

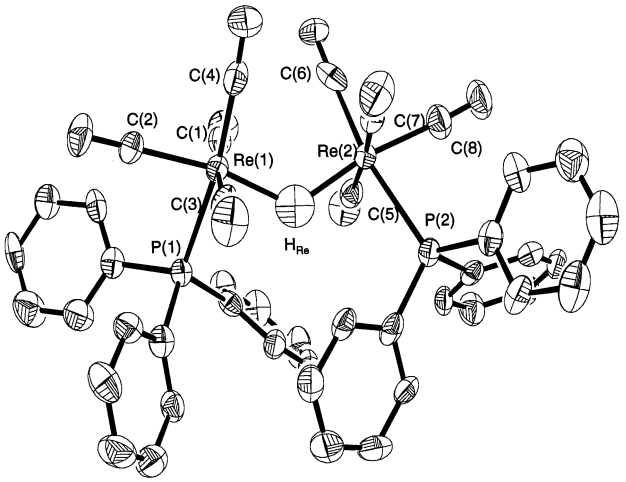

Fig. 4. ORTEP diagram for {[*cis*-$Re(CO)_4(PPh_3)]_2(\mu\text{-}H)$}{$BAr_F$} (**4a′**), BAr_F^- not shown, 50% probability ellipsoids.

Et_3SiMe as the major product in the recovered volatiles from the reaction mixture. The heterolytic cleavage of SiH in this system occurs very much like the H_2 reactions described above. However, a silicon cation equivalent 'Et_3Si^+' (silylium ion [47]) is produced instead of H^+, which then goes on to react with either ReMe in **1**, or the anion $MeB(C_6F_5)_3^-$. There was no evidence for the formation of either methane or a silicon-bridged dimer (Eq. (11)).

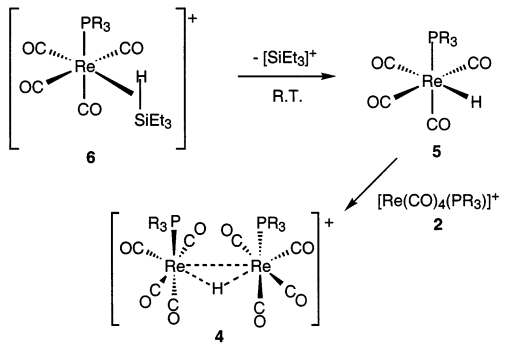

(11)

The reaction was also carried out using the BAr_F^- derivative to see if the σ-complex would be stable at room temperature, and if not, what sort of Si containing products would be formed. When one equiv. of Et_3SiH was injected into a cooled (−40°C) CD_2Cl_2 solution of [*cis*-$Re(CO)_4(PPh_3)(ClCD_2Cl)$][$BAr_F$] formation of the σ-complex [*cis*-$Re(CO)_4(PPh_3)(\eta^2\text{-}HSiEt_3)$][$BAr_F$] (**6a′**) was observed, and the hydride region of the ^1H NMR spectrum is shown in Fig. 5. However, warming of the sample to room temperature for 5 min still resulted in the complete conversion to the hydride-bridged dimer **4a′**. GC/MS analysis of the volatiles from this reaction revealed the presence of the disiloxane $Et_3SiOSiEt_3$, Et_3SiF, and 1,3-$(CF_3)_2(C_6H_4)$. This suggests that the $Re(\eta^2\text{-}HSiEt_3)$ complex is unstable at room temperature even with the non-interacting anion BAr_F^-, and that elimination of Et_3Si^+ probably proceeds with fluoride abstraction from the BAr_F^- anion as observed for other incipient silylium ions [47]. The silicon cation equivalent Et_3Si^+ which is eliminated in these reactions probably exists as a highly reactive solvento complex instead of a bare Si^+ cation. Closely paralleling **6**, $[IrH_2(\eta^2\text{-}HSiEt_3)_2(PPh_3)_2]SbF_6$ also forms Et_3SiF and a hydride-bridged dimer on warming to 25°C [48]. As pointed out by Luo et al., the Si atom of the Si–H bond is highly activated toward nucleophilic attack because of depletion of the electron density of the Si–H bond on coordination to cationic metals. Cationic silane complexes generally cannot be isolated even if they do not attack the anion. For example $[CpFe(CO)(PEt_3)(\eta^2\text{-}HSiEt_3)]BF_4$ is readily hydrolyzed by trace water to Et_3SiOH and $[CpFe(CO)(PEt_3)(\eta^2\text{-}H_2)]BF_4$ [49].

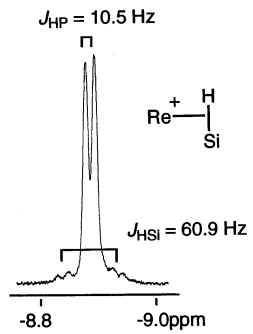

Fig. 5. ^1H NMR (CD_2Cl_2, −20°C) of [*cis*-$Re(CO)_4(PR_3)(\eta^2\text{-}HSiEt_3)$][$BAr_F$] (**6a′**), hydride region.

It is important to note that the σ silane complexes **6** were formed in complete conversion at low temperature in the NMR spectra in CD_2Cl_2 solution, whereas the H_2 complexes **3** were only observed in low concentrations (< 5%) due to fast exchange with free methylene chloride in CD_2Cl_2 solution. This indicates that tertiary SiH is a better ligand than H_2 (and CH_2Cl_2) towards [*cis*-$Re(CO)_4(PR_3)]^+$. This is in agreement with the notion that the greater basicity of the Si–H bond compared to the H–H bond makes Si–H a better σ donor [1d], assuming that σ donation is the much greater bonding component in the Re system. Thus silanes appear to be electronically both better σ-donors and π-acceptors in comparison to H_2 (as previously conjectured [1d,f]). Steric effects are however much greater for silanes and more congested first-row fragments such as $Mn(CO)_3(PCy_3)_2$ and $[Mn(CO)(diphosphine)_2]^+$ do not bind silanes [14,23e]. There are few examples in the literature of the heterolytic bond cleavage of SiH [48–50], and we have not found any other examples in which a σ-complex was observed as an intermediate in the activation. Recently, Bullock and Song [50a] have shown that $Cp(CO)_3W(FBF_3)$ reacts with Et_3SiH to produce $Cp(CO)_3WH$ (70% conversion, 45 min at 22°C). Fryzuk et al. [50b,c] have shown novel hetero-

lytic cleavage of H_2 and $BuSiH_3$ on a $Zr–N_2–Zr$ dimer, which is calculated to be exothermic by 19.7 kcal mol^{-1} for cleavage of SiH_4 [51] (Eq. (12)).

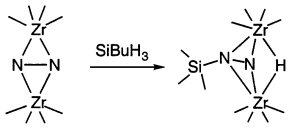

(12)

2.6. Reaction of [cis-Re(CO)$_4$(PR$_3$)(ClCH$_2$Cl)][A] with olefins

The formation of σ-complexes and subsequent heterolytic activation of HX bonds could be useful in the functionalization of olefins, such as in ionic hydrogenation or hydrosilylation. Keeping this in mind, we examined the reactivity of ethylene and *cis*-cyclooctene (cco) towards [*cis*-Re(CO)$_4$(PR$_3$)]$^+$. Placing a CH_2Cl_2 solution of [*cis*-Re(CO)$_4$(PPh$_3$)(S)][BAr$_F$] (S = Et$_2$O, CH_2Cl_2) under an atmosphere of ethylene and subsequent addition of hexanes produced the complex [*cis*-Re(CO)$_4$(PPh$_3$)(C$_2$H$_4$)][BAr$_F$] (**7**) in 74% yield (Eq. (13)). Similarly, the addition of an excess of cco to a CH_2Cl_2 solution of [*cis*-Re(CO)$_4$(PPh$_3$)(S)][BAr$_F$] and

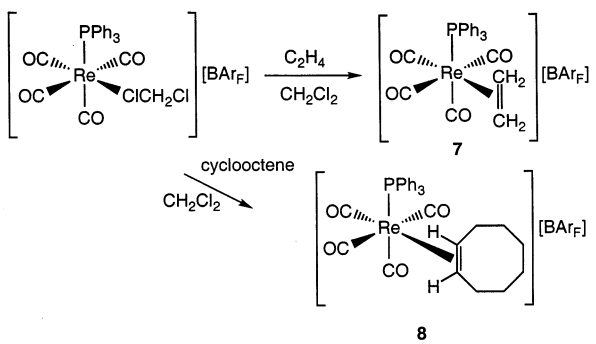

(13)

subsequent addition of hexanes provided the olefin-coordinated complex [*cis*-Re(CO)$_4$(PPh$_3$)(C$_8$H$_{14}$)][BAr$_F$] (**8**) in 72% yield. These complexes were isolated as white crystalline solids and satisfactory elemental analysis were obtained.

The bound ethylene in **7** could not be removed under vacuum, and did not exchange with CD_2Cl_2 when dissolved for NMR experiments. The ^1H showed a doublet at 4.11 ppm with $J_{HP} = 2.4$ Hz, shifted upfield from free ethylene (5.40 ppm). The $^{13}C\{^1H\}$ NMR spectrum showed only one ethylene carbon environment. If the rotation about the Re–(C$_2$H$_4$) axis could be stopped, then two resonances should be observed in the ethylene region of the ^{13}C NMR spectrum. However, the low temperature (-70°C) ^1H and $^{13}C\{^1H\}$ NMR spectra of **7** did not differ from the spectra taken at room temperature. This result suggests that the rotation about the Re–(C$_2$H$_4$) axis is not hindered by significant π-interactions between the Re d-orbitals and ethylene π* orbital, but since the ethylene is bound quite strongly, there must be considerable σ-donation from ethylene to the Re^+ center. The bound cco in **8** also could not be removed under vacuum and did not exchange with free CD_2Cl_2 in solution. The ^1H and $^{13}C\{^1H\}$ spectra for **8** at room temperature indicate four carbon and five proton environments. Finally, attempts to hydrogenate **7** or **8** with H_2 were unsuccessful due to the strong binding of the olefins versus H_2 to the Re^+ center.

3. Conclusions

The reaction of *cis*-Re(CO)$_4$(PR$_3$)Me (R = Ph, Cy) with the Lewis acid B(C$_6$F$_5$)$_3$ was studied by NMR spectroscopy and was found to provide an equilibrium mixture of the solvent coordinated complex [*cis*-Re(CO)$_4$(PR$_3$)(ClCH$_2$Cl)][MeB(C$_6$F$_5$)$_3$] and the reactants. The coordinated dichloromethane was observed in the low temperature ^{13}C NMR spectra. Reaction of *cis*-Re(CO)$_4$(PR$_3$)Me with H_2 in the presence of B(C$_6$F$_5$)$_3$ at low temperature yielded the σ-bonded [*cis*-Re(CO)$_4$(PR$_3$)(η^2-H$_2$)][MeB(C$_6$F$_5$)$_3$] which decomposed at room temperature via heterolytic cleavage of the H_2 to produce methane and the hydride-bridged dimer {[*cis*-Re(CO)$_4$(PR$_3$)]$_2$(μ-H)}{MeB(C$_6$F$_5$)$_3$} (**4**). Similarly, [*cis*-Re(CO)$_4$(PR$_3$)(ClCH$_2$Cl)][A] reacted with Et_3SiH to form the σ-silane complex. The Re(η^2-HSiEt$_3$)$^+$ complex is observed at low temperature, but decomposes at room temperature to form the thermodynamically-favored hydride-bridged dimer and 'Et_3Si^+', which is not observed, but reacts further to form methyl, fluoride, and siloxane products via heterolytic cleavage of the Si–H bond. The silane complex is somewhat more stable than the H_2 complex, indicating that silanes are better σ-donors (in addition to being better π-acceptors) than H_2. Finally, the olefins reacted in this study bind quite strongly to this Re^+ system, and the rotation about the Re–olefin bond could not be stopped at low temperature, indicating strong σ and only weak π interactions between the olefin and the Re center.

The H_2 binding and heterolytic cleavage on this and other highly electrophilic organometallic complexes that contain strong π-acceptor CO ligands can be directly related to the structure and function of metalloenzymes such as Fe-containing hydrogenases that catalyze $H_2 \leftrightarrow 2H^+ + 2e^-$. The latter have surprisingly been found to contain electrophilic dinuclear active sites that are organometallic in character with CO ligands which would promote binding and heterolytic cleavage of molecular H_2. The M–M bonds (Fe–Fe or Fe–Ni) in hydrogenases appear to be an important structural component and are likely sites for reversible protonation to form a bridging hydride as the initial step in one mechanism of H_2 formation that is pro-

posed here. Even when no other bridging ligands or metal bonds are present, electrophilic systems appear to favor formation of hydride-bridged complexes such as **4** rather than mononuclear hydrides. No matter which mechanism of the many possible for hydrogenase function ultimately proves to be correct, it is clear that several principles from organometallic H_2 binding and activation directly come into play. Perhaps a more proper viewpoint is that once again Nature is billions of years ahead of us in designing the ideal sites for activation of H_2 and other small molecules.

4. Experimental

4.1. General considerations

NMR spectra were measured on a Varian UNITY series 300 MHz spectrometer. FT-IR spectra were obtained on a Nicolet Magna 750 spectrometer. Solvents were dried either by distillation from P_2O_5 (CH_2Cl_2, NC_5F_5), Na/benzophenone (Et_2O, hexanes), or by elution from columns of activated alumina and BTS catalyst according to the procedure describe by Grubbs and coworkers [52]. NMR solvents were dried over either CaH_2 or P_2O_5 and vacuum transferred before use. ^1H NMR spectra were referenced to either $CHDCl_2$ or TMS, ^{31}P NMR spectra were referenced to H_3PO_3, and ^{13}C spectra were referenced to CD_2Cl_2 or CH_2Cl_2. The BAr_F^- and $B(C_6F_5)_3$ peaks are not reported in the ^{13}C NMR data and are virtually identical to those reported previously, regardless of the cationic fragment [12,21]. All manipulations and reactions with air sensitive compounds were carried out either in a Vacuum Atmospheres He Drybox or under Ar using standard Schlenk techniques. The $B(C_6F_5)_3$ [53], **1a** [11], **1b** [8], *cis*-$Re(CO)_4(PCy_3)Cl$ [8], **5a** [54] and [*cis*-$Re(CO)_4(PR_3)(ClCH_2Cl)][BAr_F]$ [8] were prepared as described previously. The $H(BEt_3)Li$, Et_3SiH and *cis*-cyclooctene (cco) were purchased from Aldrich.

4.2. Reaction of cis-$Re(CO)_4(PR_3)Me$ ($R = Ph$, **1a**; Cy, **1b**) with $B(C_6F_5)_3$

The addition of **1a** (0.031 g, 0.054 mmol) to a CD_2Cl_2 solution of $B(C_6F_5)_3$ (0.028 g, 0.054 mmol) in an NMR tube provided a colorless solution. ^1H NMR (24°C, CD_2Cl_2) 7.3–8.0 (m, 15H, Ph), 0.48 (br s, 1.3H, BMe), −0.56 (br s, 1.7H, ReMe). $^{31}P\{^1H\}$ NMR (24°C, CD_2Cl_2) 11.1, 10.4 (br, overlapping). ^1H NMR (−70°C, CD_2Cl_2) 7.3–8.0 (m, 15H, Ph), 0.44 (s, 3H, BMe). $^{31}P\{^1H\}$ NMR (−70°C, CD_2Cl_2) 11.1. $^{13}C\{^1H\}$ NMR (−70°C, CH_2Cl_2) 184.09 (d, $J_{CP} = 8.5$, CO), 181.52 (d, $J_{CP} = 41.8$, CO), 180.60 (d, $J_{CP} = 6.2$, CO), 132.77 (d, $J_{CP} = 11.0$, Ph), 132.57 (s, Ph), 129.81 (d, $J_{CP} = 11.0$, Ph), 127.98 (d, $J_{CP} = 52.8$, Ph), 67.0 (s, $ReClCH_2Cl$), 9.4 (BMe). Thermodynamic data were calculated using the integration between BMe and ReMe peaks in the ^1H NMR spectra recorded at 23.8, 11.1, 2.3, −4.4, −11.3, −19.5 and −27.1°C, with a CH_3OH capillary insert for temperature calibration.

Similarly, **1b** (0.021 g, 0.035 mmol) was added to a CD_2Cl_2 solution of $B(C_6F_5)_3$ (0.018 g, 0.035 mmol) in an NMR tube to provide a colorless solution. ^1H NMR (24°C, CD_2Cl_2) 1.0–2.2 (m, 33H, Cy), 0.22 (v br, 3H, BMe + ReMe). $^{31}P\{^1H\}$ NMR (24°C, CD_2Cl_2) 25.2 (br). ^1H NMR (−70°C, CD_2Cl_2) 1.0–2.2 (m, 33H, Cy), 0.42 (s, 3H, BMe). $^{31}P\{^1H\}$ NMR (−70°C, CD_2Cl_2) 25.4.

4.3. NMR reactions with H_2, HD, and D_2

In a typical experiment, a J-Young NMR tube was charged with CD_2Cl_2 (0.5 ml) or C_6D_5F (**1**) (0.0100 g), and 1 equiv. of $B(C_6F_5)_3$. The solution was then frozen at liquid N_2 temperature, backfilled with approximately 3 atm of H_2, and closed off. The NMR tube was then immediately transferred to the pre-cooled NMR probe (−80°C), and spectra were collected as the sample was warmed to room temperature in 10 or 20°C increments.

4.4. Preparation of cis-$Re(CO)_4(PCy_3)(H)$ (**5b**)

An aliquot of $HBEt_3$ in Et_2O (0.91 ml, 1.0 M) was added to a stirred and cooled (−78°C) solution of *cis*-$Re(CO)_4(PCy_3)Cl$ (0.556 g, 0.905 mmol) in Et_2O (40 ml). The reaction mixture was stirred for 5 min, then slowly warmed to room temperature and stirred for 30 min. To the resulting pale yellow reaction mixture, CH_2Cl_2 (0.50 ml) was added to quench any unreacted $HBEt_3$. The solvents were removed under vacuum and the residue was dissolved in benzene (10 ml) and filtered under Ar through a fine frit. The benzene was removed under vacuum and the residue chromatographed on SiO_2 (8 g) eluting with hexanes. The first fraction was collected and removal of volatiles provided **5b** as a white solid (0.23 g, 43% yield). *Anal.* Calc. for $C_{22}H_{34}O_4PRe$: C, 45.58; H, 5.91. Found: C, 45.38; H, 5.94%. FT-IR (cm^{-1}, Nujol, ν(CO)) 2073 (m), 1980 (s), 1962 (s), 1951 (s). ^1H NMR (C_6D_6), 1.82 (m, 6H, Cy), 1.73 (m, 3H, Cy), 1.64 (m, 6H, Cy), 1.51 (br s, 3H, Cy), 1.38 (m, 6H, Cy), 1.06 (m, 9H, Cy) −5.48 (d, $J_{HP} = 21.9$, 1H, ReH). $^{31}P\{^1H\}$ NMR (C_6D_6) 27.3. $^{13}C\{^1H\}$ NMR (C_6D_6) 191.84 (d, $J_{CP} = 7.4$, CO), 191.77 (d, $J_{CP} = 9.8$, CO), 189.34 (d, $J_{CP} = 38.9$, CO), 36.93 (d, $J_{CP} = 22.8$, Cy), 30.43 (s, Cy), 27.97 (d, $J_{CP} = 10.3$, Cy), 26.90 (s, Cy).

4.5. Preparation of {[cis-$Re(CO)_4(PR_3)]_2(\mu$-H)}{BAr_F} ($R = Ph$, **4a′**; Cy, **4b′**)

Diethyl ether (3 ml) was added to a vial containing **1a** (0.029 g, 0.050 mmol) and $[H(OEt_2)_2][BAr_F]$ (0.051 g, 0.050 mmol). After stirring for 1 min, **5a** (0.028 g, 0.050

mmol) was poured in and the colorless reaction mixture was stirred for 5 min before the addition of hexanes (3 ml). The solution was stored at room temperature overnight to provide large, colorless crystals of **4a′** which were washed twice with hexanes and dried in vacuo (0.091 g, 92% yield). *Anal.* Calc. for $C_{76}H_{43}BF_{24}O_8P_2Re_2$: C, 45.98; H, 2.18. Found: C, 45.57; H, 1.94%. FT-IR (cm^{-1}, Nujol, ν(CO)) 2120 (m), 2100 (w), 2035 (s), 2025 (vs), 2017 (s), 2010 (m), 1999 (m), 1979 (s). ^1H NMR (CD_2Cl_2) 7.73 (s, 8H, BAr_F), 7.3–7.6 (m, 34H, Ph + BAr_F), −15.56 (t, J_{HP} = 10.0, μ-H). $^{13}P\{^1H\}$ NMR (CD_2Cl_2) 1.9. $^{31}C\{^1H\}$ NMR (CD_2Cl_2) 184.90 (d, J_{CP} = 8.55, CO), 181.39 (d, J_{CP} = 43.26, CO), 179.98 (d, J_{CP} = 8.30, CO), 133.73 (d, J_{CP} = 11.1, Ph), 132.88 (s, Ph), 131.27 (d, J_{CP} = 49.9, Ph), 130.14 (d, J_{CP} = 10.4, Ph).

The PCy_3 analogue was prepared in a similar manner from **1b**, $[H(OEt_2)_2][BAr_F]$, and **5b** and isolated in 82% yield. *Anal.* Calc. for $C_{76}H_{79}BF_{24}O_8P_2Re_2$: C, 45.15; H, 3.94. Found: C, 45.04; H, 4.01%. FT-IR (cm^{-1}, Nujol, ν(CO)) 2111 (m), 2095 (m), 2019, 2009, 1999, 1974, 1968 (s, overlapping). ^1H NMR (CD_2Cl_2) 7.73 (s, 8H, BAr_f), 7.58 (s, 4H, BAr_F), 0.80–2.25 (m, 66H, Cy), −17.59 (t, J_{HP} = 7.8, μ-H). $^{13}P\{^1H\}$ NMR (CD_2Cl_2) 13.7. $^{31}C\{^1H\}$ NMR (CD_2Cl_2) 186.82 (d, J_{CP} = 8.5, CO), 181.64 (d, J_{CP} = 40.0, CO), 180.73 (d, J_{CP} = 7.6, CO), 37.84 (d, J_{CP} = 23.5, Cy), 30.13 (s, Cy), 27.88 (d, J_{CP} = 10.4, Cy), 26.39 (s, Cy).

4.6. X-ray structure of *4a′*

A colorless, triangular shaped crystal was mounted from a pool of mineral oil under argon gas flow on a thin glass fiber with silicon grease, and placed under a liquid nitrogen stream on a Siemens P4/PC diffractometer. The radiation used was graphite monachromatized Mo Kα radiation (λ = 0.71069 A). The lattice parameters were optimized from a least-squares calculation on 25 carefully centered reflections of high Bragg angle. The data were collected using ω scans with a 0.86° scan range. Three check reflections monitored every 97 reflections showed no systematic variation of intensities. Lattice determination and data collection were carried out using XSCANS Version 210b software. All data reduction, including Lorentz and polarization corrections and structure solution and graphics were performed using SHELXTL PC Version 4.2/360 software. The structure refinements were performed using SHELX 93 software [55]

The structure was solved using Patterson and difference Fourier techniques. These solutions yielded the two rhenium atoms and the majority of all other non-hydrogen atom positions. Subsequent Fourier synthesis gave all remaining non-hydrogen atom positions. The bridging hydride was found after all other non-hydrogen atoms had been identified and refined anisotropically. The atomic coordinates of the hydride were refined with a set isotopic temperature factor (0.08 $Å^2$). The phenyl rings of the triphenylphosphine ligands were refined as rigid bodies with the C–C distances fixed at 1.39 Å. The hydrogen atoms were fixed in positions of ideal geometry, with a C–H distance of 0.93 Å and refined using the riding model in the HFIX facility in SHELX 93. These idealized hydrogen atoms had their isotropic temperature factors fixed at 1.2 times the equivalent isotropic U of the carbon atom they were bonded to.

4.7. NMR reactions with Et_3SiH

A CD_2Cl_2 solution of **1a** (0.0157 g, 0.027 mmol) and $B(C_6F_5)_3$ (0.014g, 0.027 mmol) was transferred to an NMR tube fitted with a screw-top septa cap and cooled to −78°C. An aliquot of Et_3SiH (5 μl, 0.03 mmol) was injected and the NMR tube was immediately placed in the pre-cooled probe. The ^1H and $^{31}P\{^1H\}$ spectra were recorded at 10°C intervals between −40 and 20°C. After warming to room temperature, the volatiles were vacuum-transferred to a sample tube and analyzed by GC/MS and showed Et_3SiMe (M^+ 130) as the major product and $Et_3SiOSiEt_3$ (M^+ 246), Et_3SiCl (M^+ 150) and $(C_6H_4)(CF_3)_2$ (M^+ 214) as minor products. Similarly, Et_3SiH was added to a cooled (−78°C) solution of $[cis\text{-}Re(CO)_4(PPh_3)(ClCH_2Cl)][BAr_F]$ in CD_2Cl_2 and the reaction monitored by ^1H and $^{31}P\{^1H\}$ NMR spectroscopy. ^1H NMR (CD_2Cl_2, −40°C) 7.73 (s, 8H, BAr_F), 7.3–7.6 (m, 34H, Ph + BAr_F), 0.5–1.2 (m, 15H, SiEt), −8.89 (d, J_{HP} = 10.5, J_{HSi} = 60.9, 1H, η^2-HSi). $^{31}P\{^1H\}$ (CD_2Cl_2, −40°C) 7.2. The GC/MS of the volatiles after warming to room temperature showed $Et_3SiOSiEt_3$ as the major product and Et_3SiF (M^+ 134) and $(C_6H_4)(CF_3)_2$ as minor products.

In a similar manner, Et_3SiH was reacted with either **1b** and $B(C_6F_5)_3$, or $[cis\text{-}Re(CO)_4(PCy_3)(ClCH_2Cl)][BAr_F]$ in CD_2Cl_2 solution. The resulting NMR spectra and GC/MS data were similar to those described for the Ph derivative. ^1H NMR (CD_2Cl_2, −40°C) 7.73 (s, 8H, BAr_F), 0.8–2.2 (m, 48H, SiEt + PCy), −9.41 (d, J_{HP} = 9.3, J_{HSi} = 61.6, 1H, η^2-HSi). $^{31}P\{^1H\}$ (CD_2Cl_2, −40°C) 27.2.

4.8. Preparation of *[cis-Re(CO)$_4$(PPh$_3$)(C$_2$H$_4$)][BAr$_F$]* (7)

A Schlenk flask was charged with $[cis\text{-}Re(CO)_4(PPh_3)(OEt_2)][BAr_F]$ (0.261 g, 0.174 mmol) and placed under an atmosphere of ethylene. Methylene chloride (5.0 ml) was added and the colorless solution was stirred with vortexing for 10 min. After this time, the volume was reduced by one-third under vacuum and 20 ml of hexanes were added dropwise with constant stirring, resulting in the precipitation of white microcrys-

tals. The solution was syringed off, and the white solid washed twice with hexanes and dried in vacuo (0.190 g, 74% yield). *Anal.* Calc. for $C_{56}H_{31}BF_{24}O_4PRe$: C, 46.33; H, 2.15. Found: C, 46.14; H, 2.15%. FT-IR (cm^{-1}, Nujol, ν(CO)) 2128 (m), 2054, 2041, 2027, 2115, 1996, 1984 (s, overlapping). ^1H NMR (CD_2Cl_2) 7.73 (s, 8H, BAr_F), 7.3–7.6 (m, 34H, Ph + BAr_F), 4.11 (d, $J_{HP} = 2.4$, C_2H_4). $^{13}P\{^1H\}$ NMR (CD_2Cl_2) 2.4. $^{31}C\{^1H\}$ NMR (CD_2Cl_2) 182.44 (d, $J_{CP} = 8.8$, CO), 181.98 (d, $J_{CP} = 8.0$, CO), 178.17 (d, $J_{CP} = 42.8$, CO), 133.4 (d, $J_{CP} = 2.5$, Ph), 133.08 (d, $J_{CP} = 10.7$, Ph), 130.65 (d, $J_{CP} = 10.6$, Ph), 129.18 (d, $J_{CP} = 51.8$, Ph), 74.84 (s, C_2H_4).

4.9. Preparation of [cis-$Re(CO)_4(PPh_3)(C_8H_{14})$][$BAr_F$] (8)

In the dry box, cco (g, mmol) was added to a solution of **1a** (0.021 g, 0.036 mmol) and [Ph_3C][BAr_F] (0.039 g, 0.035 mmol) in CH_2Cl_2 (5.0 ml). After stirring for 5 min, 10 ml of hexanes were added and the reaction mixture was placed in a −30°C freezer for 1 h. The resulting pale yellow crystals were collected, washed twice with hexanes, and dried in vacuo (0.040 g, 72% yield). *Anal.* Calc. for $C_{62}H_{41}BF_{24}O_4PRe$: C, 48.55; H, 2.69. Found: C, 48.90; H, 2.68%. FT-IR (cm^{-1}, Nujol, ν(CO)). ^1H NMR (CD_2Cl_2) 7.73 (s, 8H, BAr_F), 7.3–7.6 (m, 34H, Ph + BAr_F), 4.43 (m, 2H, olefinic cco), 2.60 (m, 2H, CCO), 2.18 (m, 2H, cco), 1.84 (m, 2H, cco), 1.2–1.5 (m, 6H, cco) $^{13}P\{^1H\}$ NMR (CD_2Cl_2) 6.4. $^{31}C\{^1H\}$ NMR (CD_2Cl_2) 186.02 (d, $J_{CP} = 8.8$, CO), 182.69 (d, $J_{CP} = 7.6$, CO), 180.43 (d, $J_{CP} = 47.6$, CO), 133.33 (s, Ph), 133.20 (d, $J_{CP} = 10.4$, Ph), 130.50 (d, $J_{CP} = 10.4$, Ph), (*ipso*-Ph not observed), 101.40 (s, olefinic cco), 32.50 (s, cco), 30.01 (s, cco), 25.56 (s, cco).

5. Supplementary material

X-ray crystallographic files in CIF format for the structure determination of {[*cis*-$Re(CO)_4(PPh_3)]_2$(μ-H)}{BAr_f} are available on request from the authors.

Acknowledgements

This work is supported by the Department of Energy, Office of Basic Energy Sciences, Chemical Sciences Division. J. Huhmann-Vincent is grateful to the Director of the Los Alamos National Laboratory for postdoctoral funding. We are grateful for helpful discussions with Dr John Peters at Utah State regarding the structure and possible mechanisms of Fe hydrogenases.

References

[1] Reviews: (a) J.J. Schneider, Angew. Chem., Int. Ed. Engl. 35 (1996) 1068. (b) D.M. Heinekey, W.J. Oldham, Jr., Chem. Rev. 93 (1993) 913. (c) P.G. Jessop, R.H. Morris, Coord. Chem. Rev. 121 (1992) 289. (d) R.H. Crabtree, Angew. Chem., Int. Ed. Engl. 32 (1992) 789. (e) G.J. Kubas, Acc. Chem. Res. 21 (1988) 120. See also: (f) M.D. Butts, G.J. Kubas, X.-L. Luo, J.C. Bryan, Inorg. Chem. 36 (1997) 3341. (g) J. Li, R.M. Dickson, T. Ziegler, J. Am. Chem. Soc. 117 (1995) 11482. (h) J. Li, T. Ziegler, Organometallics 15 (1996) 3844. (i) S. Dapprich, G. Frenking, Angew. Chem., Int. Ed. Engl. 34 (1995) 354. (j) R.H. Morris, Can. J. Chem. 74 (1996) 1907. (k) J. Huhmann-Vincent, B.L. Scott, G.J. Kubas, J. Am. Chem. Soc. 120 (1998) 6808. (l) X.-L. Luo, G.J. Kubas, C.J. Burns, J. Eckert, Inorg. Chem. 33 (1994) 5219. (m) D.M. Heinekey, C.E. Radzewich, M.H. Voges, B.M. Schomber, J. Am. Chem. Soc. 119 (1997) 4172. (n) G. Frenking, U. Pidum, J. Chem. Soc., Dalton Trans. (1997) 1653.

[2] G.J. Kubas, R.R. Ryan, B.I. Swanson, P.J. Vergamini, H.J. Wasserman, J. Am. Chem. Soc. 108 (1986) 7000.

[3] (a) X.-L. Luo, G.J. Kubas, C.J. Burns, J.C. Bryan, C.J. Unkefer, J. Am. Chem. Soc. 117 (1995) 1159. (b) X.-L. Luo, G.J. Kubas, J.C. Bryan, C.J. Burns, C.J. Unkefer, J. Am. Chem. Soc. 116 (1994) 10312.

[4] D.G. Gusev, D. Nietlispach, I.L. Eremenko, H. Berke, Inorg. Chem. 32 (1993) 3628.

[5] (a) T.P. Fong, A.J. Lough, R.H. Morris, A. Mezzetti, E. Rocchini, P. Rigo, J. Chem. Soc., Dalton Trans. (1998) 2111. (b) C. Bianchini, S. Moneti, M. Peruzzini, F. Vizza, Inorg. Chem. 36 (1997) 5818.

[6] (a) J.W. Peters, W.N. Lanzilotta, B.J. Lemon, L.C. Seefeldt, Science 282 (1998) 1853. (b) Y. Nicolet, C. Piras, P. Legrand, C.E. Hatchikian, J.C. Fontecilla-Camps, Structure 7 (1999) 13. (c) M. Frey, Struct. Bonding 90 (1998) 97. (d) For overview see: M.W.W. Adams, E.I. Stiefel, Science 282 (1998) 1842.

[7] (a) G.J. Kubas, C.J. Burns, G.R.K. Khalsa, L.S. Van Der Sluys, G. Kiss, C.D. Hoff, Organometallics 11 (1992) 3390. (b) A.C. Albeniz, D.M. Heinekey, R.H. Crabtree, Inorg. Chem. 30 (1991) 3632.

[8] J. Huhmann-Vincent, B.L. Scott, G.J. Kubas, Inorg. Chem. 38 (1999) 115.

[9] S.A. Brewer, L.A. Buggey, J.H. Holloway, E.G. Hope, J. Chem. Soc., Dalton Trans. (1995) 2941.

[10] W. Beck, M. Schweiger, Z. Anorg. Allg. Chem. 595 (1991) 203.

[11] R.J. McKinney, H.D. Kaesz, J. Am. Chem. Soc. 97 (1975) 3066.

[12] X. Yang, C.L. Stern, T.J. Marks, J. Am. Chem. Soc. 116 (1994) 10015.

[13] R. Baumann, W.M. Davis, R.R. Schrock, J. Am. Chem. Soc. 119 (1997) 3830.

[14] A. Toupadakis, G.J. Kubas, W.A. King, B.L. Scott, J. Huhmann-Vincent, Organometallics 17 (1998) 5315.

[15] (a) T.S. Peng, C.H. Winter, J.A. Gladysz, Inorg. Chem. 33 (1994) 2534. (b) J.M. Fernández, J.A. Gladysz, Organometallics 8 (1989) 207. (c) C.H. Winter, J.A. Gladysz, J. Organomet. Chem. 354 (1988) C33.

[16] For a review on the coordination chemistry of halocarbons, see: R.J. Kulawiec, R.H. Crabtree, Coord. Chem. Rev. 99 (1988) 89.

[17] T.D. Newbound, M.R. Colsman, M.M. Miller, G.P. Wulfsberg, O.P. Anderson, S.H. Strauss, J. Am. Chem. Soc. 111 (1989) 3762.

[18] D. Huang, J.C. Huffman, J.C. Bollinger, O. Eisenstein, K.G. Caulton, J. Am. Chem. Soc. 119 (1997) 7398.

[19] J. Forniés, F. Martínez, R. Navarro, E.P. Urriolabeitia, Organometallics 15 (1996) 1813.

[20] B.A. Arndtsen, R.G. Bergman, Science 270 (1995) 1970.

[21] M.D. Butts, B.L. Scott, G.J. Kubas, J. Am. Chem. Soc. 118 (1996) 11831.

[22] W. Beck, K.Z. Schloter, Naturforsch., Teil B 33 (1978) 1214.

[23] (a) W.A. King, X.-L. Luo, B.L. Scott, G.J. Kubas, D.W. Zilm, J. Am. Chem. Soc. 118 (1996) 6782. (b) C.E. Forde, S.E. Landau, R.H. Morris, J. Chem. Soc., Dalton Trans. (1997) 1663. (c) G. Albertin, S. Antoniutti, M. Bettiol, E. Bordignon, F. Busatto,

Organometallics 16 (1997) 4959. (d) E. Rocchini, A. Mezzetti, H. Ruegger, U. Burckhardt, V. Gramlich, A. Del Zotto, P. Martinuzzi, P. Rigo, Inorg. Chem. 36 (1997) 711. (e) W.A. King, B.L. Scott, J. Eckert, G.J. Kubas, Inorg. Chem. 38 (1999) 1069. (f) P.I. Amrhein, S.D. Drouin, C.E. Forde, A.J. Lough, R.H. Morris, J. Chem. Soc., Chem. Commun. (1996) 1665.

[24] (a) P.A. Maltby, M. Schlaf, M. Steinbeck, A.J. Lough, R.H. Morris, W.T. Klooster, T.F. Koetzle, R.C. Srivastava, J. Am. Chem. Soc. 118 (1996) 5396. (b) T.A. Luther, D.M. Heinekey, Inorg. Chem. 37 (1998) 127.

[25] G. Perdoncin, G. Scorrano, J. Am. Chem. Soc. 99 (1997) 6983.

[26] M.S. Chinn, D.M. Heinekey, N.G. Payne, C.D. Sofield, Organometallics 8 (1989) 1824.

[27] For a review of heterolytic H_2 activation, see: P.J. Brothers, Prog. Inorg. Chem. 28 (1981) 1.

[28] R.H. Crabtree, Inorg. Chim. Acta 125 (1986) L7.

[29] (a) M. Frey, Struct. Bonding (Berlin) 90 (1998) 98. (b) S.P.J. Albracht, Biochim. Biophys. Acta 1188 (1994) 167.

[30] R.K. Thauer, A.R. Klein, G.C. Hartmann, Chem. Rev. 96 (1996) 3031.

[31] G.A. Olah, N. Hartz, G. Rasul, G.K.S. Prakash, J. Am. Chem. Soc. 117 (1995) 1336.

[32] (a) J. Cioslowski, G. Boche, Angew. Chem., Int. Ed. Engl. 36 (1997) 107. (b) J.H. Teles, S. Brode, A. Berkessel, J. Am. Chem. Soc. 120 (1998) 1345. (c) A.P. Scott, B.T. Golding, L. Radom, New. J. Chem. 22 (1998) 1171.

[33] (a) R.P. Happe, W. Roseboom, A.J. Pierek, S.P.J. Albracht, K.A. Bagley, Nature 85 (1997) 126. (b) A.J. Pierek, W. Roseboom, R.P. Happe, K.A. Bagley, S.P.J. Albracht, J. Biol. Chem. 274 (1999) 3331.

[34] (a) D.J. Darensbourg, J.H. Reibenspies, C.-H. Lai, W.-Z. Lee, M.Y. Darensbourg, J. Am. Chem. Soc. 119 (1997) 7903. (b) H.-F. Hsu, S.A. Koch, C.V. Popescu, E. Munck, J. Am. Chem. Soc. 119 (1997) 8371.

[35] (a) M. Pavlov, P.E.M. Siegbahn, M.R.A. Blomberg, R.H. Crabtree, J. Am. Chem. Soc. 120 (1998) 548. (b) S. Niu, L.M. Thomson, M.B. Hall, J. Am. Chem. Soc. 121 (1999) 4000. (c) P. Amara, A. Volbeda, J.C. Fontecilla-Camps, M.J. Field, J. Am. Chem. Soc. 121 (1999) 4468.

[36] L. De Gioia, P. Fantucci, B. Guigliarelli, P. Bertrand, Inorg. Chem. 38 (1999) 2658.

[37] L.S. Van Der Sluys, M.M. Miller, G.J. Kubas, K.G. Caulton, J. Am. Chem. Soc. 113 (1991) 2513.

[38] (a) P.J. Vergamini, G.J. Kubas, Prog. Inorg. Chem. 21 (1976) 261. (b) N.G. Connelly, L.F. Dahl, J. Am. Chem. Soc. 92 (1970) 7472.

[39] (a) D.-H. Lee, B.P. Patel, E. Clot, O. Eisenstein, R.H. Crabtree, Chem. Commun. (1999) 297. (b) A.J. Lough, S. Park, R. Ramachandran, R.H. Morris, J. Am. Chem. Soc. 116 (1994) 8356. (c) A.J. Lough, R.H. Morris, Organometallics 15 (1996) 4423.

[40] P.J. Vergamini, R.R. Ryan, G.J. Kubas, J. Am. Chem. Soc. 98 (1976) 1980.

[41] (a) Y. Higuchi, T. Yagi, N. Yasuoka, Structure 5 (1997) 1671. (b) A. Volbeda, E. Garcin, C. Piras, A.L. de Lacey, V.M. Fernandez, E.C. Hatchikian, M. Frey, J.C. Fontecilla-Camps, J. Am. Chem. Soc. 118 (1996) 12989. (c) Y. Higuchi, H. Ogata, K. Miki, N. Yasuoka, T. Yagi, Structure 7 (1999) 549.

[42] L.S. Van Der Sluys, K.A. Kubat-Martin, G.J. Kubas, K.G. Caulton, Inorg. Chem. 30 (1991) 306.

[43] C. Nataro, R.J. Angelici, Inorg. Chem. 37 (1998) 2975, and references therein.

[44] D.C. Harris, H.B. Gray, Inorg. Chem. 14 (1975) 1215.

[45] (a) K. Fauvet, R. Mathieu, R. Poilblanc, Inorg. Chem. 15 (1976) 976. (b) M.S. Arabi, R. Mathieu, R. Poilblanc, J. Organomet. Chem. 177 (1979) 199.

[46] C. Fan, M. Teixeira, J. Moura, I. Moura, B.-H. Huynh, J. LeGall, H.D. Peck Jr., B.M. Hoffman, J. Am. Chem. Soc. 113 (1991) 20.

[47] (a) C.A. Reed, Acct. Chem. Res. 31 (1998) 325. (b) M. Kira, T. Hino, H. Sakurai, J. Am. Chem. Soc. 114 (1992) 6697. (c) J.B. Lambert, S.Z. Zhang, S.M. Ciro, Organometallics 13 (1994) 2430.

[48] X.-L. Luo, R.H. Crabtree, J. Am. Chem. Soc. 111 (1989) 2527.

[49] E. Scharrer, S. Chang, M. Brookhart, Organometallics 14 (1995) 5686.

[50] (a) R.M. Bullock, J.-S. Song, J. Am. Chem. Soc. 116 (1994) 8602. (b) M.D. Fryzuk, J.B. Love, S.J. Rettig, V.G. Young, Science 275 (1997) 1445. (c) H. Basch, D.C. Musaev, K. Morokuma, M.D. Fryzuk, J.B. Love, W.W. Seidel, A. Albinati, T.F. Koetzle, W.T. Klooster, S.A. Mason, J. Eckert, J. Am. Chem. Soc. 120 (1999) 523.

[51] H. Basch, D.C. Musaev, K. Morokuma, M.D. Fryzuk, J.B. Love, W.W. Seidel, A. Albinati, T.F. Koetzle, W.T. Klooster, S.A. Mason, J. Eckert, J. Am. Chem. Soc. 120 (1999) 523.

[52] A.B. Pangborn, M.A. Giardellow, R.H. Grubbs, R.K. Rosen, F.J. Timmers, Organometallics 15 (1996) 1518.

[53] A.G. Massey, A.J. Park, J. Organomet. Chem. 5 (1966) 218.

[54] J.G. Stack, R.D. Simpson, F.J. Hollander, R.G. Bergman, C.H. Heathcock, J. Am. Chem. Soc. 112 (1990) 2716.

[55] XSCANS and SHELXTL PC are products of Siemens Analytical X-ray Instruments, Inc., 6300 Enterprise Lane, Madison, WI 53719. G.M. Sheldrick, SHELX-93 is a program for crystal structure refinement, University of Göttingen, Germany, 1993.